PERGAMON

Journal of Structural Geology 25 (2003) 253–262

JOURNAL OF STRUCTURAL GEOLOGY

www.elsevier.com/locate/jsg

Polyphase deformation of mylonites from the Renco gold mine (Zimbabwe): identified by crystallographic preferred orientation of quartz

Jochen Kolb[a,*], Alexander F.M. Kisters[b], F. Michael Meyer[a], Heinrich Siemes[a]

[a]*Institut für Mineralogie und Lagerstättenlehre, RWTH Aachen, Wüllnerstr. 2, D-52056 Aachen, Germany*
[b]*Department of Geology, University of Stellenbosch, Private Bag X1, Matieland 7602, South Africa*

Received 22 February 2001; received in revised form 4 February 2002; accepted 4 February 2002

Abstract

Gold mineralization at Renco mine in the Northern Marginal Zone of the Limpopo Belt, Zimbabwe, is hosted by a set of intersecting steep and shallow dipping shear zones, locally termed 'reefs'. Both steep and shallow reefs are closely associated with quartz-mylonites. The crystallographic preferred orientation of quartz from samples of these quartz-mylonites indicate that deformation in steep reefs occurred under amphibolite-facies conditions. Pole figures and microstructures of samples from shallow reefs, in contrast, show evidence for an origin of the auriferous mylonites at amphibolite-facies conditions that were subsequently overprinted by deformation under lower-greenschist-facies conditions. Since mineralization is hosted by both reef geometries, gold mineralization is inferred to have occurred during deformation and associated fluid infiltration along mylonites at amphibolite-facies grades, coeval with Late-Archaean thrusting of rocks of the Northern Marginal Zone onto rocks of the Zimbabwe Craton.

The crystallographic preferred orientation patterns of quartz point to a normal sense of movement during reactivation of the shallow reefs, probably related to the Meso-Proterozoic tectonometamorphic event that has affected the central parts of the Limpopo Belt at ca. 2.0 Ga. Normal faulting along the boundary between the Northern Marginal Zone and Zimbabwe Craton has, to date, not yet been documented, and may provide some important constraints for the understanding of the kinematics of the Meso-Proterozoic tectonics in the Limpopo Belt.

Keywords: Polyphase deformation; Mylonites; Crystallographic preferred orientation

1. Introduction

The microstructural development and crystallographic preferred orientation (CPO) of mineral fabrics and minerals provide a powerful tool for our understanding of the kinematics of deformation and P–T–t paths of complexly deformed metamorphic terrains (e.g. Lister and Price, 1978; Lister and Dornsiepen, 1982; Lister and Snoke, 1984; Schmid and Casey, 1986; Kruhl, 1986, 1991; Pryer, 1993; Lloyd and Freeman, 1994; Wenk, 1994; Joy and Saha, 1998, 2000). Quartz, in particular, is an important mineral for the investigation of deformation paths since it not only plays a major role for the rheological behavior of crustal rocks, but also because it is stable under most metamorphic conditions and displaying a variety of intracrystalline deformation textures. Microstructures in quartz such as undulose extinction, subgrain formation, etc. are easily recognized under the microscope. However, in order to obtain information on the different temperature-sensitive slip systems of quartz, one has to determine its CPO.

The CPO of quartz is controlled by different slip systems. At lower temperatures (lower-greenschist facies) and faster strain rates, basal ⟨a⟩ slip is the dominant mechanism. This causes a c-axis fabric maximum near the Z-axis of the finite strain ellipsoid ($X \geq Y \geq Z$) (Bouchez and Pêcher, 1981; Schmid and Casey, 1986). With increasing temperature, rhombohedral ⟨a⟩ slip becomes important in mid-greenschist facies environments, yielding c-axis maxima at an intermediate orientation between the Y- and Z-axes. The prism ⟨a⟩ slip system operates at even higher temperatures and slower strain rates in the amphibolite facies resulting in a c-axis maximum near the Y-axis (Bouchez and Pêcher, 1981; Lister and Dornsiepen, 1982; Mainprice et al., 1986; Schmid and Casey, 1986; Wenk, 1994). At very high temperatures (e.g. >700 °C) prism ⟨c⟩ slip becomes active in quartz (Mainprice et al., 1986; Kruhl, 1996).

In this paper, we present CPO data of quartz from quartz-mylonites that are spatially closely associated with auriferous reef structures of the Renco lode-gold deposit. The timing,

* Corresponding author. Tel.: +49-241-8095773; fax: +49-241-8092153.
E-mail address: kolb@rwth-aachen.de (J. Kolb).

0191-8141/02/$ - see front matter
PII: S0191-8141(02)00031-7

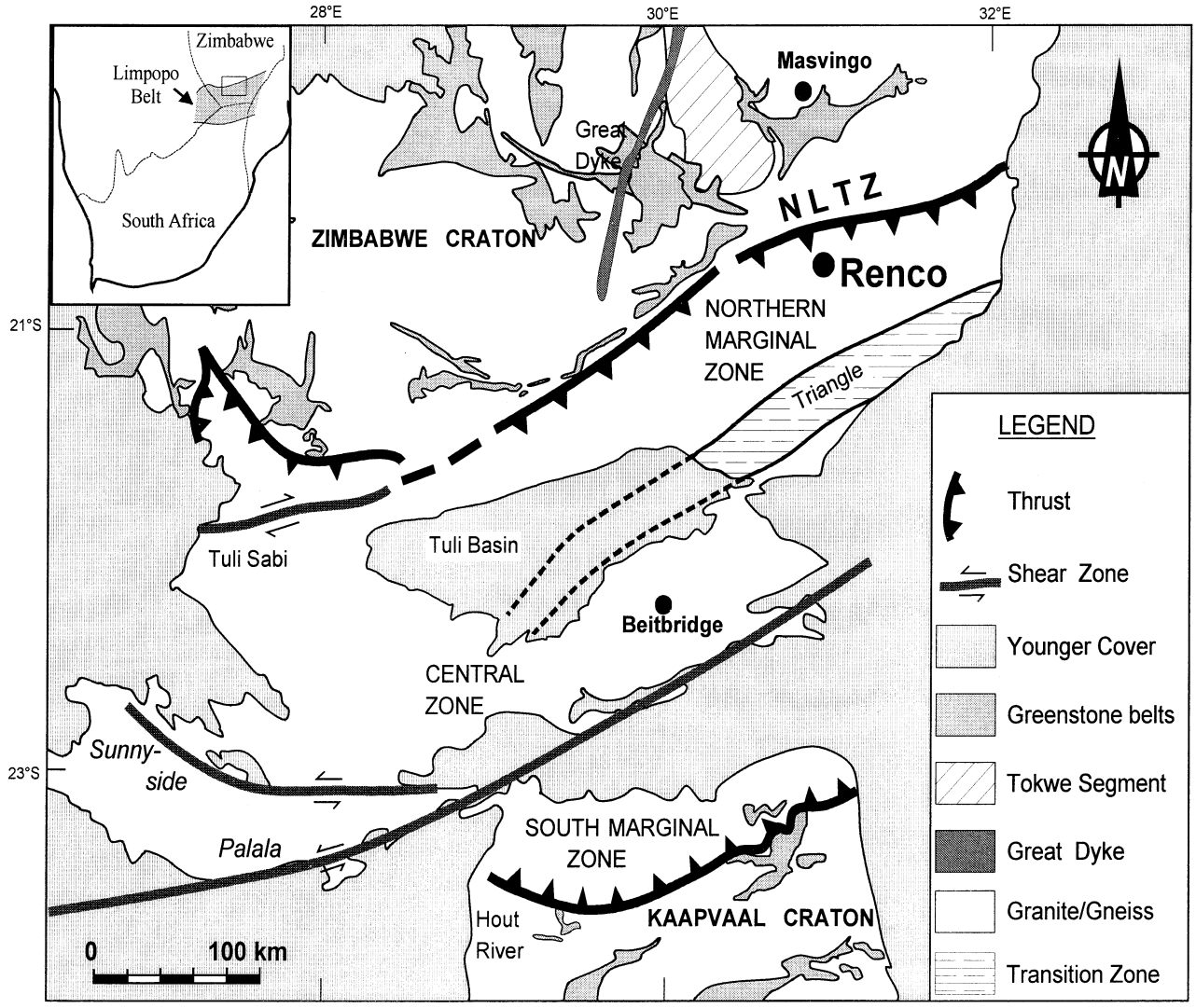

Fig. 1. Schematic geological map of the Limpopo Belt and bordering cratons, showing the Renco Mine in the Northern Marginal Zone close to the North Limpopo Thrust Zone (NLTZ), which separates the Zimbabwe Craton from the Limpopo Belt (modified after Kisters et al., 2000)

origin, and conditions of gold mineralization at Renco have been the subject of some debate in the literature and were related to either high-grade metamorphic, upper-amphibolite-facies conditions during the main phase of Late-Archaean thrusting by Kisters et al. (1997, 1998, 2000) and Kolb et al. (2000), or to greenschist-facies retrogression and associated deformation of the rocks during Meso-Proterozoic tectonism in the Limpopo Belt at ca. 2.0 Ga (Tabeart, 1989; Blenkinsop and Frei, 1996, 1997). The microstructural and CPO data presented in this paper will be used to distinguish high-grade metamorphic shearing from deformation under retrograde conditions and to constrain the timing of gold mineralization with respect to deformation.

2. Regional geology

The Renco gold mine is situated in the Northern Marginal Zone (NMZ) of the Limpopo Belt in southern Zimbabwe (Fig. 1). The NMZ is a granulite facies terrain and consists mainly of plutonic charnockites and enderbites (Kamber and Biino, 1995; Rollinson and Blenkinsop, 1995) that intruded between 2.72 and 2.62 Ga into a supracrustal sequence possibly older than 3.25 Ga (Berger et al., 1995; Berger and Rollinson, 1997). Intrusion was followed by thrusting of the high-grade terrain of the NMZ onto low- to medium-grade rocks of the Zimbabwe Craton along the North Limpopo Thrust Zone. North-northwest directed thrusting was diachronous and progressed from west to east probably between 2.67 and 2.52 Ga (Frei et al., 1999). Peak metamorphic conditions during this time reached ca. 800 °C and 800 MPa in the east and 600 MPa in the west (Rollinson, 1989; Tsunogae et al., 1992; Kamber and Biino, 1995) and were followed by exhumation and retrogression of the NMZ to amphibolite-facies grade (Ridley, 1992; Kolb et al., 2000) at temperatures of ca.

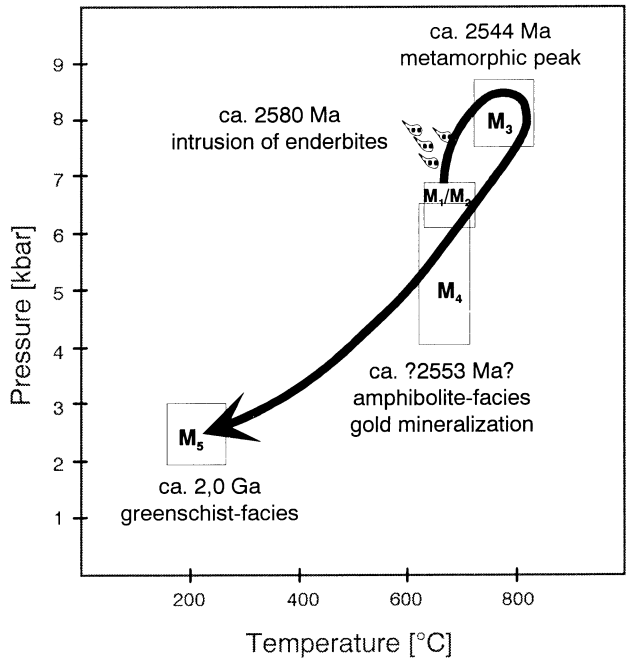

Fig. 2. *P–T* path calculated from petrologic investigations at Renco, showing the main tectonometamorphic events (modified after Kolb, 2000). M_x refers to the different stages of metamorphism. Used geothermobarometers for the different stages: $M_{1/2}$: garnet–clinopyroxene–quartz–plagioclase (Kolb, 2000); M_3: garnet–orthopyroxene (Rollinson, 1989); M_4: garnet–orthopyroxene rims (Rollinson, 1989), garnet–biotite, oxygen isotopes (Kolb et al., 2000); M_5: prehnite–laumontite–calcite–quartz paragenesis (Kolb, 2000).

600–700 °C and pressures of 400–650 MPa (Fig. 2; Rollinson, 1989; Tsunogae et al., 1992). Recent works have emphasized the overprint of Late-Archaean structures in the Limpopo Belt by a Meso-Proterozoic ca. 2.0 Ga tectonometamorphic event. This Meso-Proterozoic tectonism is reflected by high-grade metamorphism and deformation in the Central Zone of the Limpopo Belt and a greenschist-facies overprint and associated brittle–ductile faulting in rocks of the NMZ further north (Fig. 2; Kamber and Biino, 1995; Blenkinsop and Frei, 1996, 1997). However, the actual kinematics and extent of this overprint in the NMZ are still poorly constrained.

3. Mine geology

The Renco mine is located in an ovoid-shaped, enderbitic intrusion some 10 km to the south of the contact of the NMZ and the Zimbabwe Craton, within shallow-dipping gneisses of the North Limpopo Thrust Zone (Fig. 1). The host-rock enderbites display magmatic textures and are composed of quartz, plagioclase, alkali feldspar, orthopyroxene, clinopyroxene, and biotite as the main constituents with accessory green hornblende, garnet, apatite, zircon, and opaques. Gold mineralization at Renco is hosted by a shear-zone system that is considered to be synchronous with Late-Archaean, regional-scale thrusting along the North Limpopo Thrust Zone under upper-amphibolite-facies conditions (Kisters et al., 1998, 2000; Kolb et al., 2000). The gold mineralized shear zone system at Renco is characterized by a set of narrow (0.5–3-m-wide) intersecting shear zones. Shallow reefs show a variety of strike directions between NNE–SSW and ENE–WSW, and dip, on average, 25° to the south. Steep reefs are near vertical, E–W striking, pipe-like lodes which plunge at about 25° to the east. The cross-cutting relationships between steep and shallow reef structures and the similar petrographic development of the two reef geometries provide evidence of their contemporaneous formation (Kisters et al., 1998; Kolb et al., 2000). Macroscopic and microscopic shear sense indicators (foliation drag, rolling and *S–C* structures) from shallow reefs yield a predominant top-to-the-NNW thrust sense of movement. Kinematic indicators in steep reefs indicate a north-up sense of movement, which Kisters et al. (1998, 2000) interpret to represent an origin as R_2-Riedel shears that formed during thrusting along shallow reefs.

Both steep and shallow reefs show a characteristic internal zonation that includes: (1) amphibolite-facies quartz–feldspar–biotite–hornblende mylonites that bound the mineralized reefs against relatively undeformed wall-rock enderbites, (2) locally developed quartz-mylonites, and (3) sulfide-rich lithons in the central parts of the reef structures forming up to 50-m-long (both down-dip and along strike) and 0.5-m-wide lensoid bodies surrounded by quartz–feldspar–biotite–hornblende- and quartz-mylonites. These lithons are characterized by an amphibolite-facies garnet–quartz–biotite–alkalifeldspar alteration paragenesis and contain the bulk of gold–sulfide mineralization (Kisters et al., 2000; Kolb et al., 2000). Structurally, lithons are characterized by fracture networks of different macroscopic and microscopic vein geometries filled with mainly sulfides and, locally, fine specks of free gold. Larger fractures contain implosion breccias, made up of angular clasts of wall rock cemented by a sulfide matrix. Brittle fracture networks in lithons together with the pervasive ductile deformation of alteration parageneses indicate the overall brittle–ductile style of deformation in lithons (Kisters et al., 2000). When present, the quartz-mylonites are located between the quartz–feldspar–biotite–hornblende mylonites and the lithons. The contacts between the quartz-mylonites and the lithons are sharp but contacts between the quartz-mylonites and the quartz–feldspar–biotite–hornblende mylonites may be gradational. In the latter case, quartz-mylonites show strongly laminated textures and form part of the amphibolite-facies, ductile shear-zone system in both shallow and steep reefs.

4. Analytical procedure

A total of 200 oriented thin sections were investigated by optical microscopy for their mineralogical composition and

Table 1
Location, description, and photograph of the samples used for the pole figures. Photographs were taken from the polished specimens used for texture goniometry analysis

No.	Reef type	Location	Description		Photograph
715	Shallow reef	Level 540/759 south drive	Red (main) reef: transition of quartz–feldspar–biotite–hornblende-mylonites to quartz-mylonites; two different macroscopic textures of quartz-mylonites	Dark gray part; ~10 vol.% feldspar (arrow), 10 vol.% sulfides, aligned parallel to foliation; dominated by Qtz_2, Qtz_1, present	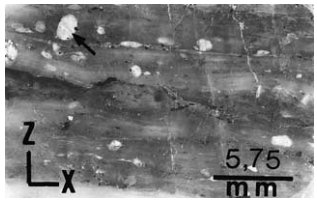
716	Shallow reef	Level 540/759 south drive		Dark milky part; only minor saussuritized feldspar (arrow); dominated by Qtz_2	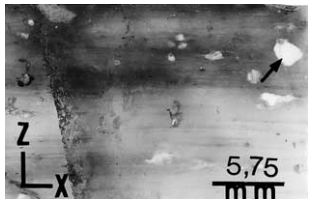
717	Steep reef	Level 480/63 raise	50 cm section through the complete reef: quartz-mylonites in the hanging wall and the footwall of the lithon	Milky gray quartz-mylonite; hanging wall, minor sulfides (arrow) and chlorite, no feldspar; dominated by Qtz_1	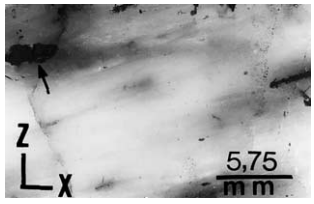
718	Steep reef	Level 480/63 raise		Milky quartz-mylonite from the footwall, minor chlorite (arrow) and feldspar, very rare sulfides; dominated by Qtz_1	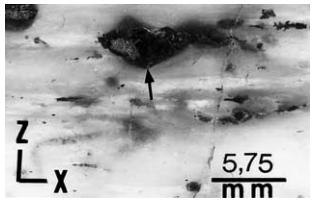
719	Shallow reef	Level 480/60 stope	Red (main) reef: transition from the strongly silicified quartz-mylonite to the sulfide-rich lithon	Dark gray part, 3 vol.% feldspar, 5 vol.% sulfides, aligned parallel to foliation; dominated by Qtz_2	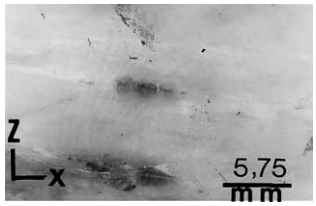
720	Shallow reef	Level 480/60 stope	Same reef as 719 but about 100 m up dip	White milky quartz-mylonite, very rare feldspar, chlorite and sulfides; dominated by Qtz_2	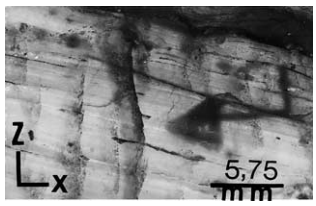

microscopic shear sense indicators. From these, six samples of quartz-mylonites were chosen for analysis of CPO, four samples (nos. 715, 716, 719 and 720) from shallow reefs and two of them (nos. 717 and 718) from steep reefs (Table 1).

The pole figures were determined by a Philips PW1710 X-ray texture goniometer using samples of 13 × 23 mm and 2–4.5 mm thick. Measurement conditions for Cu-Kα radiation are 35 kV, 30 mA and a Ni-filter was used. Step width was

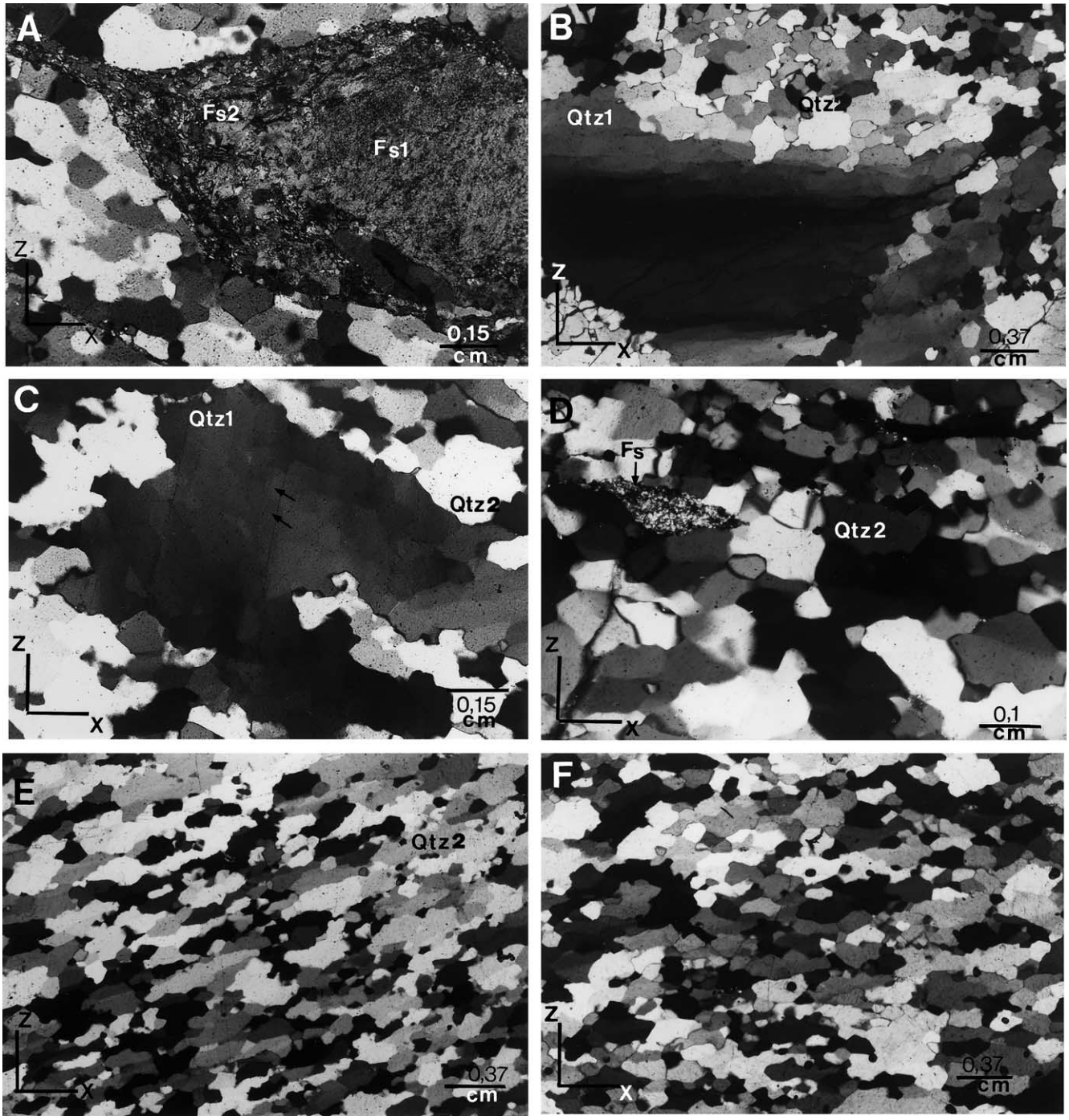

Fig. 3. Photomicrographs of the different samples (crossed polarized light), showing the microtextures of quartz and feldspar: (A) sample 715: two generations of feldspar ($Fs_{1/2}$) almost completely saussuritized, Fs_1 is recrystallized dynamically to Fs_2; (B) sample 717, steep reef: large $quartz_1$ (Qtz_1) crystal showing undulose extinction and subgrains mantled by recrystallized $quartz_2$ grains (Qtz_2); (C) sample 715, shallow reef: relic $quartz_1$ (Qtz_1) in the center, showing undulose extinction and subgrains surrounded by dynamically recrystallized $quartz_2$ (Qtz_2), subgrain boundaries marked (arrow) are prismatic because of the view almost parallel to *c*-axis (compare CPO); (D) sample 715, shallow reef: $quartz_2$ (Qtz_2) with relative straight grain boundaries and almost no internal deformation, a highly saussuritized feldspar grain (Fs) is also observable; (E) sample 719 and (F) sample 720, shallow reefs: characteristic elongate $quartz_2$ (Qtz_2) microtexture defining a strong foliation.

5° in tilt Ψ between 5° and 85°, and in azimuth Ω. The poles of prism a {110} at 18.18° Θ, prism m {100} at 10.35° Θ, rhombohedral r and z {101} at 13.23° Θ, and dipyramids {112} at 25.01° Θ were measured. The pole figures were corrected for defocussing by measurements of a quartz powder displaying random orientation. However, at a tilt-angle of $\Psi = 85°$ this correction for defocussing was likely too strong. The pole figures were transformed and smoothed

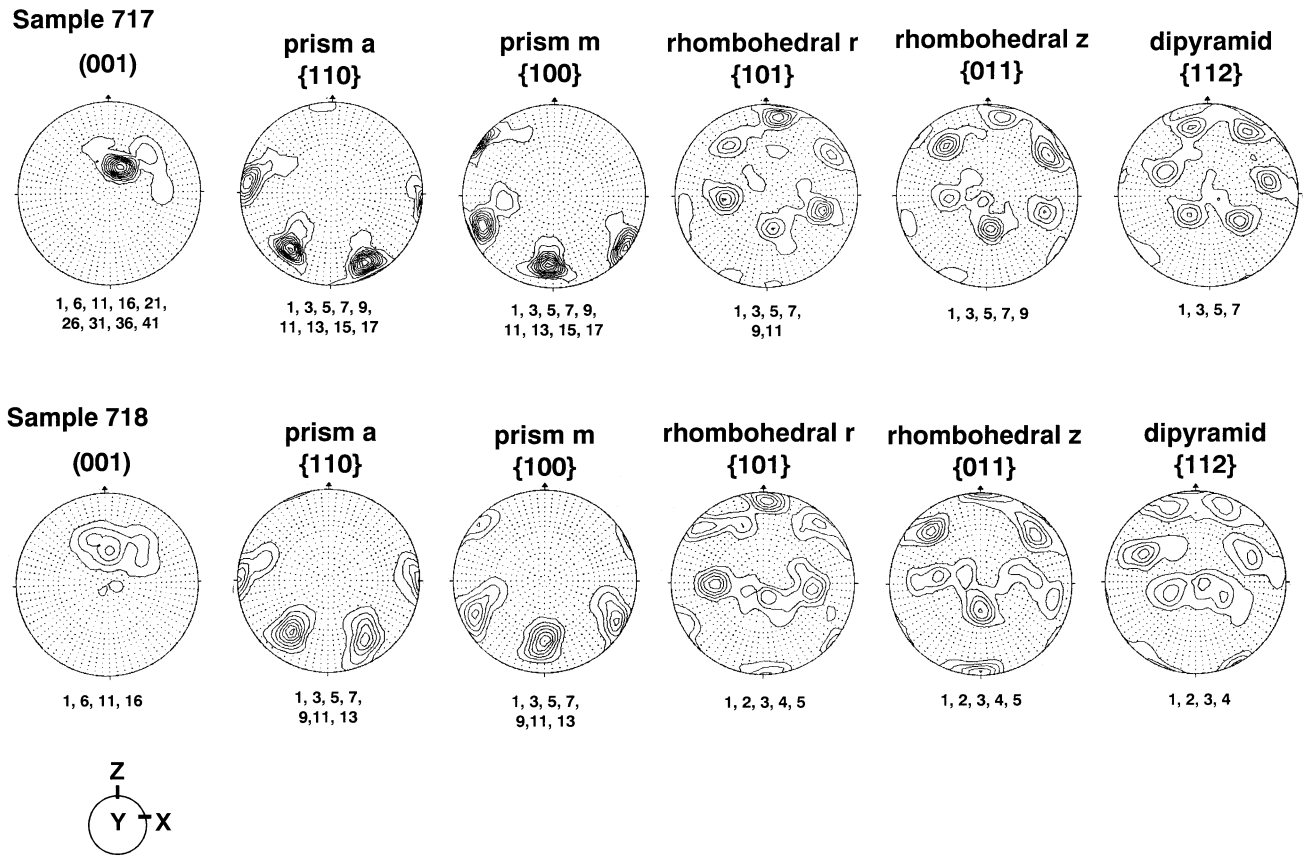

Fig. 4. Calculated and recalculated pole figures from samples from the steep reef (nos. 717 and 718) as contour plots in equal area lower hemisphere projections. Contour intervals are given below each pole figure.

by the program STARPLOT as described by Traas et al. (1994). The orientation density function (ODF) was calculated from the measured and transformed pole figures with the computer program MENTEX (Schaeben and Siemes, 1996) to an angle of 72.5° to eliminate possible problems regarding the above-mentioned correction. The pole figures for {100}, {110}, and {112} were recalculated from the measured data set. The pole figures (001), {101}, and {011} were calculated using the data set of the four measured pole figures.

5. Petrography and microstructural development of quartz-mylonites

Quartz-mylonites are mainly composed of quartz (70–95 vol.%), plagioclase (5–20 vol.%), biotite (1–10 vol.%), and sulfides (10–30 vol.%; Table 1). Minor amounts of epidote, chlorite, and carbonates are present. Accessories are apatite and zircon. In contrast to the pyrrhotite-dominated sulfide assemblage in lithons, sulfides in quartz-mylonites are mainly pyrite (80–95 vol.%) with minor amounts of chalcopyrite (2–5 vol.%) and pyrrhotite (1–3 vol.%). Gold grades are relatively low with a maximum value of 3 ppm, compared with average values of 22 ppm in lithons. Biotite ranges from 0.2 to 0.5 mm in size and its basal planes are arranged parallel to the mylonitic foliation. Two generations of plagioclase can be distinguished. The first generation is up to 0.5 mm in diameter and forms porphyroclasts. Plagioclase has been affected by pervasive crystal plastic deformation indicated by undulose extinction, subgrains, micro-shear zones with evidence of dynamic recrystallization, and core and mantle structures. The second generation of plagioclase (0.1–0.2 mm) has developed by dynamic recrystallization through both grain-boundary migration and subgrain rotation. Notably, both generations of plagioclase have been affected by a pervasive saussuritization (Fig. 3A). The greenschist-facies overprint of the amphibolite-facies mylonites is also evidenced by the replacement of hornblende by chlorite, the presence of epidote and late-stage carbonates in veins.

Quartz occurs as two generations (Fig. 3). The first generation of quartz is up to 2 mm in diameter. The crystals show lobate grain boundaries and strongly developed undulose extinction and subgrains (Fig. 3B and C). The second generation of quartz is derived from dynamic recrystallization of the first generation by both subgrain rotation and grain boundary migration (Fig. 3). The 0.15–0.25-mm-sized crystals have straight to slightly bent grain boundaries and show weak undulose extinction and rare subgrains (Fig.

3D–F). The first generation of quartz is mainly preserved in the quartz-mylonites from steep reefs (nos. 717 and 718) where larger, strongly undulose grains dominate over smaller recrystallized grains (Fig. 3B). In contrast, in samples from shallow reefs (nos. 716, 719 and 720) small, pervasively-recrystallized, second-generation quartz clearly dominates (Fig. 3E and F), except in sample no. 715 in which the two quartz generations are almost equally present (Fig. 3C and D).

6. Description of pole figures

Pole figure data for quartz-mylonites from steep and shallow reefs are presented in relation to the strain ellipsoid axes. The *X*-axis lies parallel to the stretching lineation, *Z* is perpendicular to foliation and *Y* perpendicular to *X* and *Z*. The samples were prepared in *XZ* orientation.

6.1. Steep reef

The pole figures from quartz-mylonites from a steep reef (nos. 717 and 718) are very similar (Fig. 4). They are asymmetric with respect to the chosen *XYZ* frame. This indicates that the sample was not strictly prepared perpendicular to the foliation. Taken together, a very pronounced and consistent CPO for quartz is evident. The calculated poles for (001), i.e. the *c*-axes, define a strong point maximum at ~30° to *Y*. The pole figures for the prism planes display point maxima at three orientations with the maxima for the prism 'a' lying almost perfectly between the point maxima for the prism 'm'. The CPO patterns for the rhombohedral and dipyramidal planes are more complex and show six less well defined maxima, but the pole figures display a strong consistency. An almost identical character in the preferred orientation of positive and negative forms is indicated yielding a hexagonal character, similar to specimen Gran 133 of Schmid and Casey (1986).

6.2. Shallow reef

The pole figures from quartz-mylonites (nos. 716, 719 and 720) from shallow reefs also display similar and strong CPOs which, however, are markedly different from those from steep reefs (Fig. 5). Little differences in the distribution of maxima and girdles are observed. The poles of (001) display a strong maximum close to *Z* with a small, sinistral angular departure from *Z* of 5° for sample 720, 16° for sample 716, and 20° for sample 719. This asymmetry is present in all the other pole figures and its significance is discussed below. The pole figures of the prism planes

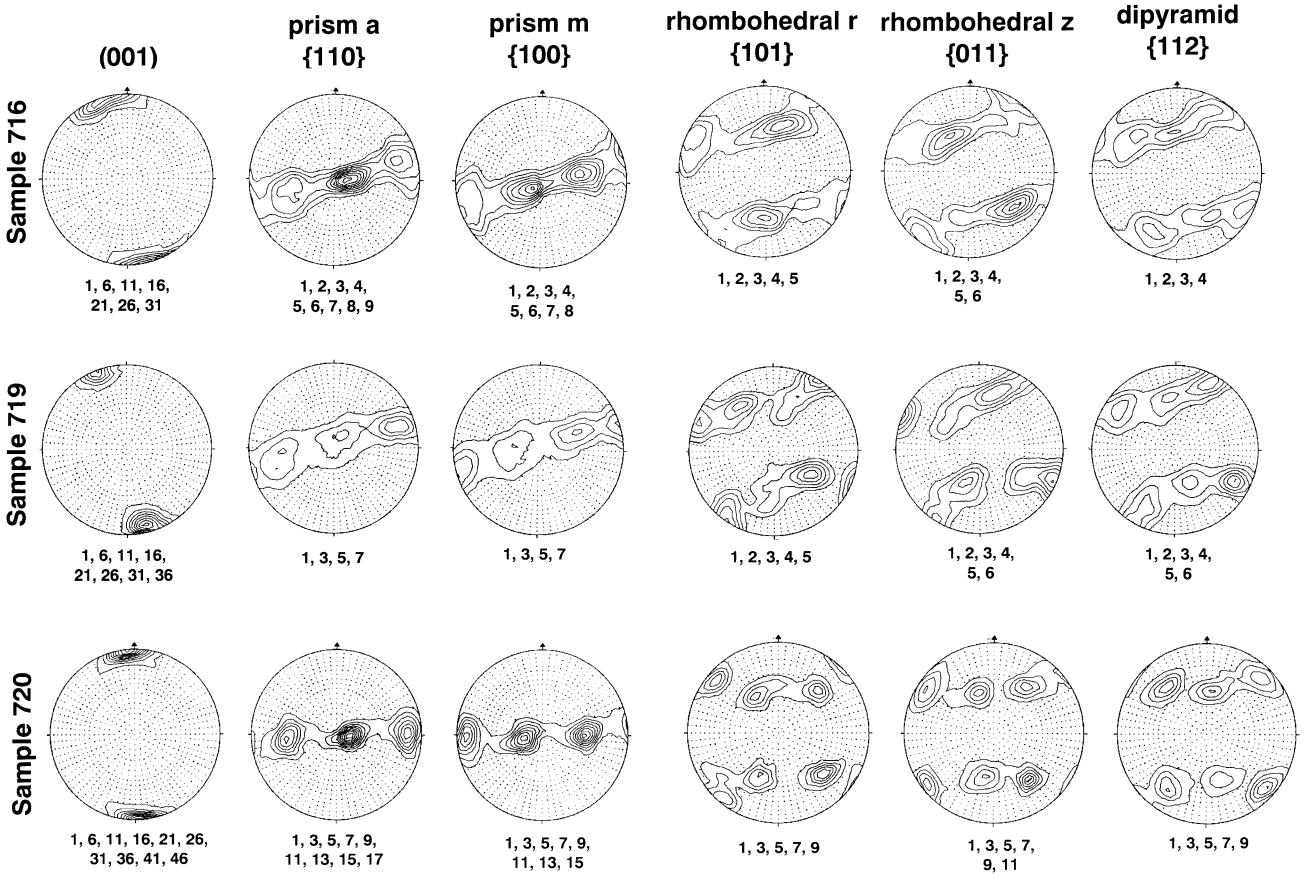

Fig. 5. Calculated and recalculated pole figures from samples from the shallow reef (nos. 716, 719 and 720) as contour plots in equal area lower hemisphere projections. Contour intervals are given below each pole figure.

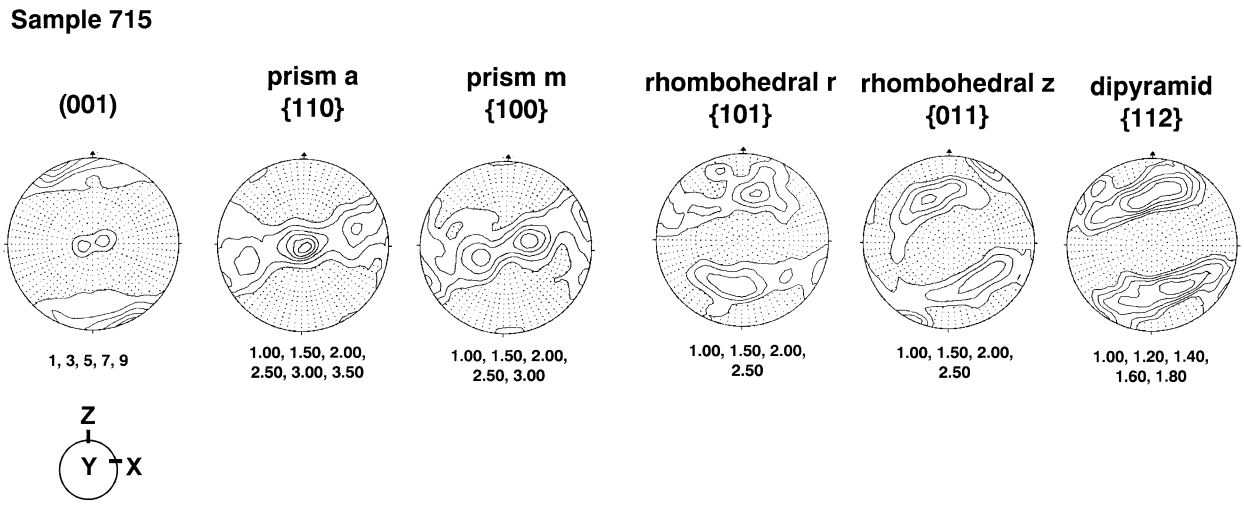

Fig. 6. Calculated and recalculated pole figures from the shallow reef sample (no. 715) as contour plots in equal area lower hemisphere projections. Contour intervals are given below each pole figure.

form single girdles, and the poles of the rhombohedral and dipyramidal planes form small circles with opening angles around *Z* varying from 100° to 140°.

The pole figures from sample 715, also a quartz-mylonite from a shallow reef, differ slightly from the latter pole figures. The maximum of (001) close to *Z* is not as pronounced and an additional maximum occurs in the centre at *Y* (Fig. 6). The poles of the prism planes show a tendency toward crossed-girdle patterns with the appearance of maxima symmetrically disposed with respect to *X*. The rhombohedral and dipyramidal planes form pole figures that somewhat differ from small circle distributions.

7. Discussion

The microstructural development and CPO of quartz are, among other parameters, temperature dependent and, thereby, provide constraints on the conditions of deformation in the auriferous mylonites of the Renco mine. From the outset, it should be emphasized that the CPO patterns from the shallow reefs cannot be derived from those of the steep reefs by simple rotation, because the pole figures for prisms, rhombohedral, and dipyramidal planes are very different, thus excluding sample misorientation problems with respect to the mineral stretching lineation.

The CPO patterns of quartz from quartz-mylonites in steep reefs (nos. 717 and 718) display a consistent asymmetry with respect to the *XYZ* frame due to misorientation during sample preparation. This leads to a rotation of the pole figures of ~30° in the *Z* direction. If this displacement is rotated back, a strong maximum for the *c*-axes close to *Y* occurs (Fig. 4). This pattern is generally attributed to crystal plastic slip in quartz on the prism planes in the ⟨a⟩ direction, which is mainly active under amphibolite-facies conditions (Lister and Dornsiepen, 1982; Mainprice et al., 1986; Schmid and Casey, 1986; Wenk, 1994). An upper temperature limit is provided by the absence of prism ⟨c⟩ slip, which limits the temperature of deformation to below ~700 °C (e.g. Kruhl, 1996). A lower temperature limit is provided by the pervasive recrystallization of feldspar in quartz-mylonites (Fig. 3A), which indicates temperatures >500–550 °C during shearing (Voll, 1976; Tullis, 1983; Stünitz and FitzGerald, 1993). The temperature interval between 500 and 700 °C overlaps exactly with geothermometric results from garnet–biotite pairs and O-isotope thermometry from the alteration paragenesis in lithons that host the gold mineralization at Renco (Kolb et al., 2000).

In contrast, specimens from the shallow reefs show a maximum of *c*-axes close to the *Z* direction (Fig. 5). This pattern, formed by the dominance of the basal ⟨a⟩ slip system, is characteristic for deformation under lower greenschist-facies conditions, at temperatures at or below ~300 °C (Bouchez and Pêcher, 1981; Schmid and Casey, 1986). These low-grade metamorphic conditions during shearing are also indicated by the almost completely saussuritized feldspars observed in the quartz-mylonites (Fig. 3B; Table 1). The pole figure of *c*-axes of sample 715 shows another maximum in *Y* similar to the mylonites from the steep reefs (Fig. 6). This quartz-mylonite no. 715 is characterized by a CPO pattern intermediate between the steep and the shallow reefs also shown by the maxima of prism planes close to *Z*.

Our investigation of the quartz CPOs correlates with the microtextural observations of two generations of quartz related to different conditions of deformation. The first generation of quartz, which characterizes the quartz-mylonites of the steep reefs, and which is partly preserved in the shallow reefs (sample 715; Fig. 3C), is ascribed to shearing under amphibolite-facies conditions. The second generation of quartz, which dominates in the shallow reefs although present in the steep reefs (Fig. 3B), is ascribed to deformation and recrystallization under lower greenschist-facies conditions. The dominance of the second generation of

quartz in the shallow reefs leads to an overall smaller grain size compared with the steep reefs (Fig. 3). Notably, the elongate nature of the second generation quartz forms a strong foliation in the shallow reef samples 716, 719 and 720 in contrast to sample 715, where the quartz grains are not very elongate. This observation agrees with the CPO data indicating only a weak greenschist-facies overprint for the shallow reef sample 715 leading to the preservation of amphibolite-facies textures (Fig. 3C–F).

The c-axes in all pole figures from shallow reefs, including sample 715, are not strictly parallel to *Z* but show a sinistral rotation about *Y* by up to 20° (Figs. 5 and 6). This asymmetry is commonly attributed to non-coaxial deformation (Lister and Dornsiepen, 1982; Bouchez et al., 1983; Schmid and Casey, 1986). The asymmetry indicates a sinistral sense of shear which, for the given orientations of the samples, points to a normal sense of shear along the shallow reefs. Considering the reverse sense of shear preserved in amphibolite-facies mylonites of the shallow reefs (Kisters et al., 1998, 2000; Kolb et al., 2000), this suggests that shallow reefs, in particular, were reactivated as normal faults during lower-greenschist facies metamorphic conditions during which the quartz fabrics recorded the relatively low-temperature strain overprint. Notably, Tabeart (1989) also recorded a normal sense of shear in the shallow reefs based on classical U-stage measurements of quartz *c*-axes. He discarded his results that were, at that time, difficult to reconcile with the thrust tectonics recorded in rocks of the NMZ.

The pole figures from the steep reefs also display a component of non-coaxial strain, which is sinistral with respect to the chosen *XYZ* frame (Fig. 4). This is in agreement with macroscopic kinematic indicators yielding a north-up sense of movement. The asymmetry of the pole figures thus supports earlier interpretations of the steep reefs being developed along R_2-Riedel shears that formed during the Late-Archaean top-to-the-NW thrust movement along shallow reefs during amphibolite facies metamorphism.

7.1. Implications for the timing of gold mineralization at Renco

The microstructure and CPO pattern of quartz in quartz-mylonites from both steep and shallow reefs at Renco show evidence of two phases of deformation that took place under amphibolite- and greenschist-facies metamorphic conditions, respectively. The fact that deformation fabrics and alteration parageneses in auriferous steep reefs record almost exclusively amphibolite-facies conditions of deformation and mineralization with only limited retrograde overprint makes an origin of gold mineralization under lower greenschist facies conditions, as postulated by Tabeart (1989) and Blenkinsop and Frei (1996, 1997), unlikely. Our data suggest that amphibolite-facies shearing and gold mineralization in the Renco reefs are related to the Late-Archaean (~2.6 Ga) regional-scale thrusting. At about 2.0 Ga, after a period of about 500 Ma of tectonic quiescence, a phase of high-grade metamorphism and tectonism in the Central Zone of the Limpopo Belt (Kamber et al., 1995) led to a contemporaneous greenschist facies reactivation of shear zones in the Transition Zone of the NMZ and at the contact of NMZ and Zimbabwe craton in the north (Kamber and Biino, 1995; Blenkinsop and Frei, 1996, 1997). The shallow reefs at Renco developed parallel to these shear zones and, hence, could easily be reactivated as normal faults under lower-greenschist facies conditions. The lack of greenschist-facies deformation fabrics in steep reefs suggests that they were misoriented with respect to the regional stress field and, thus, not reactivated to the same extent as shallow reefs.

8. Conclusions

The study of the CPOs and microstructures of quartz from quartz-mylonites associated with auriferous reef structures of the Renco mine reveals a polyphase tectonometamorphic evolution of the reefs. Both shallow and steep reef geometries originated as high-temperature, amphibolite-facies shear zones in a top-to-the-NW thrust regime, related to the Late-Archaean regional scale thrusting of the NMZ onto rocks of the Zimbabwe Craton. The microstructural observations and the CPOs presented in this paper combined with high-temperature alteration parageneses associated with the mineralized reef structures indicate that gold mineralization was associated with this Late-Archaean deformation. A subsequent deformation under lower-greenschist facies metamorphic conditions has affected, in particular, the shallow reefs. Notably, the CPOs of quartz from the shallow reefs indicate that the earlier high-temperature thrust zones were reactivated as low-angle normal faults. The presence of economic-grade gold mineralization in steep reefs that were not affected by retrogression and subsequent deformation indicates that the later, low-grade metamorphic deformation was not associated with gold mineralization. The brittle, low-angle normal faulting event is tentatively related to the ca. 2.0 Ga, Meso-Proterozoic tectonism in the Limpopo Belt, which has affected large parts of the NMZ. Normal faulting at the boundary between the NMZ and Zimbabwe Craton has, to date, not been recorded and may bear important aspects for our understanding of the nature of the Meso-Proterozoic tectonometamorphic event in the Limpopo belt.

Acknowledgements

The authors thank the mine management of the Renco Mine for their permission to publish the results of this study and the mine geologists for their support during field work. Jörg Keichel from the Institute of Physical Metallurgy and Metal Physics, RWTH Aachen, is thanked for the texture measurements and Monika Wiechert for

photographic work. Comments by J.L. Bouchez and an anonymous reviewer are greatly appreciated. Financial support of this study by the Deutsche Forschungsgemeinschaft (DFG grant Me 1425/1-1, 1-2) is gratefully acknowledged.

References

Berger, M., Rollinson, H.R., 1997. Isotopic and geochemical evidence for crust-mantle interaction during Late Archaean crustal growth. Geochimica et Cosmochimica Acta 61, 4809–4829.

Berger, M., Kramers, J.D., Naegler, T.F., 1995. Geochemistry and geochronology of charnoenderbites in the northern marginal zone of the Limpopo Belt, southern Africa, and genetic models. Schweizerische Mineralogisch Petrographische Mitteilungen 75, 17–42.

Blenkinsop, T.G., Frei, R., 1996. Archean and Proterozoic mineralization and tectonics at the Renco Mine (Northern Marginal Zone, Limpopo Belt, Zimbabwe). Economic Geology 91, 1225–1238.

Blenkinsop, T.G., Frei, R., 1997. Archean and Proterozoic mineralization and tectonics at the Renco Mine (Northern Marginal Zone, Limpopo Belt, Zimbabwe)—a reply. Economic Geology 92, 747–752.

Bouchez, J.L., Pêcher, A., 1981. The Himalayan main central thrust pile and its quartz-rich tectonites in Central Nepal. Tectonophysics 78, 23–50.

Bouchez, J.L., Lister, G.S., Nicolas, A., 1983. Fabric asymmetry and shear sense in movement zones. Geologische Rundschau 72, 401–419.

Frei, R., Blenkinsop, T.G., Schönberg, R., 1999. Geochronology of the late Archaean Razi and Chilimanzi suites of granites in Zimbabwe: implications for the late Archaean tectonics of the Limpopo Belt and Zimbabwe Craton. South African Journal of Geology 102(1), 55–63.

Joy, S., Saha, D., 1998. Influence of micaceous impurity on dynamically recrystallized quartz *c*-axis fabric in L–S tectonites from the Singhbhum Shear Zone and its footwall, Eastern India. Journal of Structural Geology 20, 1509–1520.

Joy, S., Saha, D., 2000. Dynamically recrystallized quartz *c*-axis fabrics in greenschist facies quartzites, Singhbhum shear zone and its footwall, eastern India—influence of high fluid activity. Journal of Structural Geology 22, 777–793.

Kamber, B.S., Biino, G.G., 1995. The evolution of high-T low-P granulites in the Northern Marginal Zone sensu stricto, Limpopo Belt, Zimbabwe—the case for petrography. Schweizerische Mineralogisch Petrographische Mitteilungen 75, 427–454.

Kamber, B.S., Kramers, J.D., Napier, R., Cliff, R.A., Rollinson, H.R., 1995. The Triangle shear zone, Zimbabwe, revisited: new data document an important event at 2.0 Ga in the Limpopo Belt. Precambrian Research 70, 191–213.

Kisters, A.F.M., Kolb, J., Meyer, F.M., 1997. Archean and Proterozoic mineralization and tectonics at the Renco Mine (Northern Marginal Zone, Limpopo Belt, Zimbabwe)—a discussion. Economic Geology 92, 745–746.

Kisters, A.F.M., Kolb, J., Meyer, F.M., 1998. Gold mineralization in high-grade metamorphic shear zones of the Renco Mine, southern Zimbabwe. Economic Geology 93, 587–601.

Kisters, A.F.M., Kolb, J., Meyer, F.M., Hoernes, S., 2000. Hydrologic segmentation of high-temperature shear zones: structural, geochemical and isotopic evidence from auriferous mylonites of the Renco mine, Zimbabwe. Journal of Structural Geology 22, 811–829.

Kolb, J., 2000. Tektonik, Petrographie und Geochemie goldvererzter Scherzonen der Renco Mine, Northern Marginal Zone, Limpopo Belt, Zimbabwe (Ph.D. Thesis). Aachener Geowissenschaftliche Beiträge 34. Wissenschaftsverlag Mainz, Aachen, Germany, 236pp.

Kolb, J., Kisters, A.F.M., Hoernes, S., Meyer, F.M., 2000. The origin of fluids and nature of fluid-rock interaction in midcrustal auriferous mylonites of the Renco mine, southern Zimbabwe. Mineralium Deposita 35, 109–125.

Kruhl, J.H., 1986. Textures and *c*-axis orientations of deformed quartz crystals from porphyric dikes of the Alpine "Root Zone" (Western Alps). Geologische Rundschau 75/3, 601–623.

Kruhl, J.H., 1991. Why always quartz?. Zbl. Geol. Paläont. 1, 123–137.

Kruhl, J.H., 1996. Prism- and basal-plane parallel subgrain boundaries in quartz: a microstructural geothermobarometer. Journal of Metamorphic Geology 14, 581–589.

Lister, G.S., Price, G.P., 1978. Fabric development in a quartz–feldspar mylonite. Tectonophysics 49, 37–78.

Lister, G.S., Dornsiepen, U.F., 1982. Fabric transitions in the Saxony granulite terrain. Journal of Structural Geology 4, 81–92.

Lister, G.S., Snoke, A.W., 1984. S–C mylonites. Journal of Structural Geology 6, 617–638.

Lloyd, G.E., Freeman, B., 1994. Dynamic recrystallization of quartz under greenschist facies conditions. Journal of Structural Geology 16, 867–881.

Mainprice, D., Bouchez, J.L., Blumenfeld, P., Tubia, J.M., 1986. Dominant *c*-slip in naturally deformed quartz: implications for dramatic plastic softening at high temperature. Geology 14, 819–822.

Pryer, L.L., 1993. Microstructures in feldspars from a major crustal thrust zone: the Grenville Front, Ontario, Canada. Journal of Structural Geology 15, 21–36.

Ridley, J.R., 1992. On the origins and tectonic significance of the charnockite suite of the Archean Limpopo Belt, Northern Marginal Zone, Zimbabwe. Precambrian Research 55, 407–422.

Rollinson, H.R., 1989. Garnet–orthopyroxene thermobarometry of granulites from the North Marginal Zone of the Limpopo Belt, Zimbabwe. In: Daly, J.S., Cliff, R.A., Yardley, B.W.D. (Eds.), Evolution of Metamorphic Belts. Geological Society of London Special Publication 43, pp. 331–335.

Rollinson, H.R., Blenkinsop, T.G., 1995. The magmatic, metamorphic and tectonic evolution of the Northern Marginal Zone of the Limpopo Belt in Zimbabwe. Journal of the Geological Society of London 152, 65–77.

Schaeben, H., Siemes, H., 1996. Determination and interpretation of preferred orientation with texture goniometry: an application of indicators to maximum entropy pole- to orientation-density inversion. Mathematical Geology 28, 169–201.

Schmid, S.M., Casey, M., 1986. Complete fabric analysis of some commonly observed quartz *c*-axis patterns. Geophys. Monograph. 36, 263–286.

Stünitz, H., FitzGerald, J.D., 1993. Deformation of granitoids at low metamorphic grade II: granular flow in albite-rich mylonites. Tectonophysics 221, 269–297.

Tabeart, C.F., 1989. Structural and geochemical setting of gold mineralization at Renco Mine, Zimbabwe. Ph.D. thesis, London, Imperial College, 298pp.

Traas, C., Siemes, H., Schaeben, H., 1994. Smoothing pole figures using tensor products of trigonometric and polynomial splines. Materials Science Forum 157–162, 453–458.

Tsunogae, T., Miyano, T., Harris, N.B., 1992. Metamorphic P–T profiles from the Zimbabwe craton to the Limpopo Belt, Zimbabwe. Precambrian Research 55, 259–277.

Tullis, J., 1983. Deformation of feldspars. In: Ribbe, P.H. (Ed.), Feldspar Mineralogy. Mineralogical Society of America, Reviews in Mineralogy 2, pp. 297–323.

Voll, G., 1976. Recrystallization of quartz, biotite and feldspars from Erstfeld to the Leventina Nappe, Swiss Alps, and its geological significance. Schweizerische Mineralogisch Petrographische Mitteilungen 56, 641–647.

Wenk, H.-R., 1994. Preferred orientation patterns in deformed quartzites. In: Heaney, P.J., Prewitt, C.T., Gibbs, G.V. (Eds.), Silica: Physical Behaviour, Geochemistry and Materials Applications. Reviews in Mineralogy 29, pp. 177–208.